

Alkaline degradation study of linear and network poly(ϵ -caprolactone)

J. M. Meseguer-Dueñas · J. Más-Estellés ·
I. Castilla-Cortázar · J. L. Escobar Ivirico ·
A. Vidaurre

Received: 21 June 2010 / Accepted: 25 October 2010 / Published online: 12 November 2010
© Springer Science+Business Media, LLC 2010

Abstract Alkaline hydrolysis of a polycaprolactone (PCL) network obtained by photopolymerization of a PCL macromer was investigated. The PCL macromer was obtained by the reaction of PCL diol with methacrylic anhydride. Degradation of PCL network is much faster than linear PCL; the weight loss rate is approximately constant until it reaches around 70%, which happens after approximately 60 h in PCL network and 600 h in linear PCL. Calorimetric results show no changes in crystallinity throughout degradation, suggesting that it takes place in the crystalline and amorphous phases simultaneously. Scanning electron microscopy microphotographs indicate that degradation is produced by a different erosion mechanism in both kinds of samples. The more hydrophilic network PCL would follow a bulk-erosion mechanism, whereas linear PCL would follow a surface-erosion mechanism. Mechanical testing of degraded samples shows a decline in mechanical properties due to changes in sample porosity as a consequence of the degradation process.

1 Introduction

Polycaprolactone (PCL), a biocompatible semicrystalline linear resorbable aliphatic polyester, is subject to biodegradation since its aliphatic ester bond is susceptible to hydrolysis. The field of PCL applications has expanded, due to its good processability and mechanical properties [1–3]. In the biomedical field, it is used as resorbable suture, drug delivery system [4, 5], gene carrier [6], and as scaffold for tissue engineering [7–9], applications in which long degradation times are needed.

For many applications there is a strong demand for polymers with controlled degradation properties. Many groups have studied in vitro degradation and erosion of polyesters, e.g., by means of scanning electron microscopy, gravimetric measurements, nuclear magnetic resonance, differential scanning calorimetry and X-ray diffraction [10–20]. Many different factors appear to be critical in the rate of biodegradation of polyesters and biodegradable polymers in general, but the chemical structure of the polyester is the most important factor. The presence of appropriate bonds, e.g., ester groups, capable of being cleaved by the microorganisms is crucial. Degree of crystallinity, porosity, and molecular weight seem to play an important role in the rate of degradation and the presence of more hydrophilic end groups like amino, carboxyl and hydroxyl groups also favors hydrolysis. Finally, experimental conditions such as temperature, pH, sample morphology, enzyme species and concentration, all have a particular importance [21–24].

The degradation process can be accelerated if it is performed in a basic medium. Tsuji and Ishizaka [2] studied the enzymatic and alkaline degradation of porous PCL films. Non-porous PCL samples lose 18% of their weight after 96 h in a 4 N NaOH solution at 30°C. In alkaline

J. M. Meseguer-Dueñas · J. Más-Estellés · I. Castilla-Cortázar ·
J. L. Escobar Ivirico · A. Vidaurre (✉)
Centro de Biomateriales e Ingeniería Tisular,
Universidad Politécnica de Valencia, 46022 Valencia, Spain
e-mail: vidaurre@fis.upv.es

J. M. Meseguer-Dueñas · A. Vidaurre
CIBER de Bioingeniería, Biomateriales y Nanomedicina
(CIBER-BBN), Barcelona, Spain

J. L. Escobar Ivirico
Centro de Investigación Príncipe Felipe, Autopista del Saler 16,
46013 Valencia, Spain

degradation studies, Ang et al. [3] found that the incorporation of hydroxyapatite as a filler in PCL increases degradation rate.

Aliphatic polyesters degrade *in vivo* by random hydrolytic scission of ester bonds. However, the hydrophobicity and crystallinity of poly(ϵ -caprolactone) (PCL) restrict the capacity of water to enter the structure, hence the degradation process is slow. No significant weight loss was observed until after 80 weeks of *in vivo* degradation of PCL capsules with an initial molecular weight of 55,000 g/mol [25]. In a more recent study, capsules from linear PCL with an initial molecular weight of 66,000 g/mol were implanted in rats. The capsules remained intact for 24 months and retained their mechanical strength for 30 months [26].

One of the strategies used to reduce crystallinity and increase hydrophilicity is to prepare polymer networks. Bat et al. [27] developed a method to obtain form-stable elastic networks upon gamma irradiation based on high molecular weight (co)polymers of trimethylene carbonate and (ϵ -caprolactone). The *in vitro* enzymatic erosion behavior of these hydrophobic networks was investigated using aqueous lipase solutions.

Our group recently reported a new strategy for cross-linking and hydrophilization of PCL [28]. A PCL macromer was synthesized by reacting PCL diol with methacrylic anhydride to obtain methacrylate end capped PCL. PCL networks were prepared by photopolymerization of the new macromer. The PCL macromer was copolymerized with 2-hydroxyethyl acrylate to improve the water sorption capacity of the system. The synthesis, characterization and physical properties have been described elsewhere [28, 29].

The objective of this paper was to evaluate the degradation process of PCL network as compared to linear PCL. Samples were immersed in a 5 M NaOH solution at 37°C for predetermined periods of time in order to accelerate the degradation process. Weight loss, morphology, crystallinity and mechanical properties were evaluated at various time intervals.

2 Materials and methods

2.1 Materials

α,ω -Dihydroxyl terminated PCL with molecular weight of 2000 Da and methacrylic anhydride (MA) were supplied by Aldrich. Benzoin (Scharlau, 98% pure) was employed as initiator. Dioxane (Aldrich, 99.8% pure), acetone (Aldrich, 99.5% pure), ethanol (Aldrich, 99.5% pure) and ethyl acetate anhydrous (Aldrich, 99.8%) were used as solvents. Distilled water with 10 μ S conductivity was used in the swelling studies. Linear PCL samples were obtained from

poly(caprolactone) [Polysciences (Mw 43,000–50,000)] in the form of powder without further purification.

2.2 PCL networks

The synthesis and characterization of the PCL network has been published in a previous study [28, 29]. In brief, α,ω -dihydroxyl terminated PCL was endcapped with methacrylate groups to make a polymerizable macromer. The macromer was obtained by dropping the filtrate into an excess of ethanol, filtrated, recrystallized several times and also purified by column chromatography techniques, using silica gel 60 (70–230 mesh) as stationary phase and ethyl acetate as solvent. Finally, the precipitated PCL macromer was dried at 50°C for 24 h under reduced pressure.

To obtain the PCL networks, the PCL macromer was dissolved in dioxane, 35% (w/v) and mixed with benzoin (photoinitiator, 1 wt%). The reaction was carried out through the photo-polymerization mechanism in ultraviolet light for 24 h. Low molecular weight substances were extracted by boiling in ethanol for 24 h and then drying *in vacuo* to constant weight. A film of approximately 0.8 mm thick was obtained. For the sake of comparison, linear PCL samples were obtained by melting the PCL powder onto glass plates to obtain a film of approximately 1.5 mm thick (ranging from 1.0 to 2.1 mm).

2.3 Alkaline degradation

Accelerated degradation was conducted in a highly basic medium. Specimens consisting of discs of around 5 mm diameter made from films 0.8 mm in width were placed in tubes containing a 5 M NaOH solution; the proportion sample degradation medium was 1/50 in mass. The tubes were placed in an oven at 37.0°C for predetermined periods of time. At each degradation time, triplicate samples were withdrawn, washed intensively with distilled water, wiped, weighed, and then vacuum dried prior to various analyses.

The degradation process was followed by determining the water absorption and mass loss of the materials. Samples were washed with distilled water and gently wiped with paper. Wet weight was determined in order to evaluate water uptake during hydrolysis. Percentage water sorption was determined by comparing the wet weight (w_w) at a specific time with the dry weight (w_d) according to Eq. 1

$$\text{water sorption (\%)} = \frac{w_w - w_d}{w_d} \times 100 \quad (1)$$

Percentage mass loss was determined after drying the samples under vacuum by comparing dry weight (w_d) at a specific time with the initial weight (w_0) according to Eq. 2

$$\text{weight loss (\%)} = \frac{w_0 - w_d}{w_0} \times 100 \quad (2)$$

A Mettler Toledo balance with a sensitivity of 0.01 mg was used to weigh samples.

2.4 Scanning electron microscopy (SEM)

To investigate the surface and cross section morphology of dried network samples, SEM pictures of degraded and non-degraded samples were taken using a JEOL JSM-5410 scanning electron microscope.

2.5 Differential scanning calorimetry (DSC)

The thermal properties of the samples were measured by using a Mettler Toledo differential scanning calorimeter (DSC) calibrated with indium. The measurements were carried out at a scan rate of 10°C/min between -10 and 100°C. To keep the same thermal history, each sample was first heated to 100°C and cooled down to -10 °C at a rate of -10 °C/min. Then a subsequent heating run was performed from -10 to 100°C at a rate of 10°C/min. The data from all three scans were collected for subsequent analysis. Crystallinity was calculated assuming proportionality to the experimental heat of fusion, using the reported heat of fusion of 139.5 J/g for the 100% crystalline PCL [25].

Figure 1 shows an example of the first and second heating scan measured for linear PCL after 532 h of degradation. The first scan measures the effect of the degradation process on the sample and the second analyses the melting of the crystals after the first scan had erased the previous history of the material. As all the samples were crystallized under the same conditions, the melting peak corresponding to the second heating scan depends on the material properties, not on its history.

2.6 Mechanical testing

Mechanical properties were evaluated using a Seiko TMA/SS6000 by applying three consecutive compression ramps

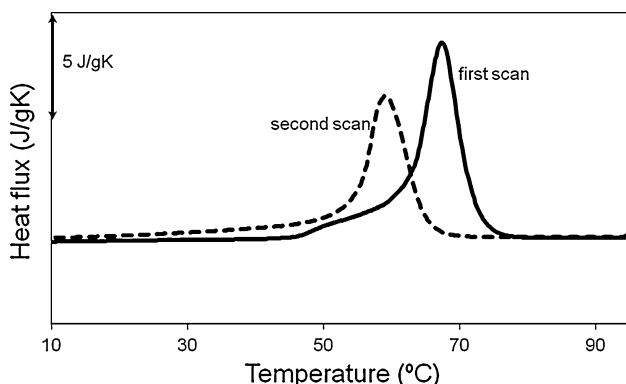


Fig. 1 Heat flux from the first and second heating scans of linear PCL after 532 h of degradation

from 1 to 400 g at 50 g/min. Sample deformation was collected every 5 s. Between each compression ramp, the sample was allowed to recover for 1 min. The section of the apparatus probe was 0.785 mm² (probe diameter 1 mm), and 5.1 MPa being the maximum value of the stress applied to samples. Three samples of each degradation time, including non-degraded samples, were measured.

3 Results and discussion

3.1 Mass loss and absorption

The structure and properties of these PCL networks have been described elsewhere [28, 29]. Overall, the melting temperature of the PCL networks was around 50°C while it was around 70°C for linear PCL; water sorption, according to Eq. 1, is around 20 and 2%, respectively (PCL network is more hydrophilic than linear PCL); while average molar mass between crosslinks equals 2,140 for PCL networks, molecular weight of linear PCL is around 45,000.

Alkaline degradation allows a comparison to be made of the degradation of network and linear PCL over a short period of time. Figure 2 presents the weight loss as a function of degrading time for PCL networks (left) and linear PCL (right). It can be observed that the samples of PCL network lost weight dramatically in the first 60 h (around 70%), while linear PCL weight loss is not even 5% in the same period. In both cases the weight loss rate is approximately constant until it reaches around 70%. This happens after approximately 60 h in the case of PCL network and after 600 h for linear PCL.

3.2 Differential scanning calorimetry (DSC)

DSC was used to monitor degree of crystallinity and thermal properties of the samples before and after degradation. Melting point (T_m) and heat of fusion (ΔH_f) were screened during the first and second heating scans.

Figure 3a and b show representative DSC thermograms of PCL networks for the first and second heating scans, respectively. The curves corresponding to the first scan present a double peak; the smaller temperature peak appears at 40°C and can be ascribed to recrystallization during degradation at 37°C. The position and size of the small peak does not change throughout degradation. On the other hand, the higher temperature peak changes in width, height and position as degradation proceeds. The peak half-width changes from 6°C for the non-degraded sample to 4°C after 42 h of degradation. Peak height changes from 6 to 10 J/g K in the same period of time. The position and width of the peak can be associated with the crystals thickness; lower melting temperatures correspond to

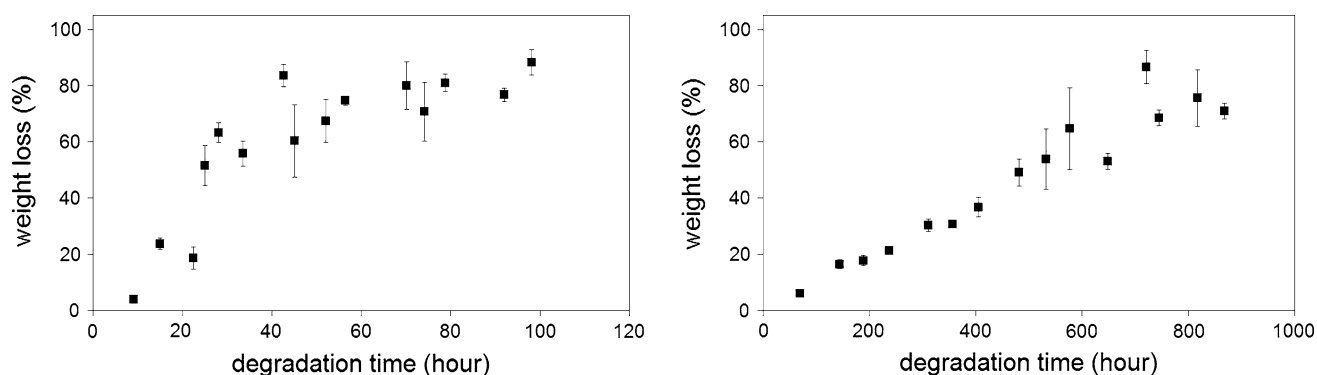


Fig. 2 Weight loss of PCL samples after alkaline degradation. *Left* PCL network. *Right* linear PCL. Every point represents the average of three samples; *error bars* are equal to standard deviation

smaller crystals thickness and smaller width corresponds to lower dispersion in crystal thickness distribution [30]. Degradation reduces the thickness of crystallites, increasing the proportion of smaller crystals, after which both temperature and peak width decline.

Figure 3 shows representative DSC thermograms of linear PCL, for the first (c) and second (d) heating scans. For this sample, only a melting peak is present. As in PCL network, peak half-width changes from 8°C for the non-degraded sample to 6°C after 532 h of degradation. Peak height changes from 5 to 9.2 J/g K after 532 h of degradation. The position of the peak moves towards lower temperatures. The effect of degradation on the crystalline phase is again the same for both kinds of samples, producing smaller crystals with lower dispersion in crystal size distribution.

The thermograms corresponding to the second heating scan are similar regardless of degradation time for both kinds of PCL samples (Fig. 3b, d). This means that even if chain scission occurs, the chain mobility that produces the crystalline structure is similar before and after degradation.

Table 1 shows the maximum melting temperature peak as a function of degrading time of PCL networks for the first (T_{m1}) and second (T_{m2}) heating scans. As stated above, the peak temperature slightly diminishes with degradation time in the first heating scan, while it remains approximately constant in the second. The crystallinity measured in the first and second heating scans are presented in Table 1. The difference between crystallinity in the first and second heating scans, 8% on average, is explained by recrystallization during storing at room temperature and degradation at 37°C. There is no appreciable change in crystallinity throughout degradation in either heating scan. This is due to degradation affecting the amorphous and crystalline phases to the same degree.

Table 2 shows the maximum melting peak temperature and crystallinity as a function of degrading time of linear PCL in the first (T_{m1} , X_1) and second (T_{m2} , X_2) heating

scans. The same main characteristics as in PCL network are present in linear PCL. The 6% average crystallinity difference measured in the first and second is lower than that obtained for the PCL network, as could be expected by the differences in melting temperatures. Melting temperature slightly diminishes with degradation time for the first heating scan, while melting temperature of the second heating scan and crystallinity in the first and second heating scans remain approximately constant. Again, crystal size diminished with degradation time and degradation had the same effect on the amorphous and crystalline phases.

By comparing the data of Tables 1 and 2 for the non-degraded samples one can see that PCL network crystallinity is 41%, much lower than that of linear PCL, 56%. This can be related to crystal size. The network structure hinders crystal formation and gives rise to smaller crystals [28]. Other studies had previously shown that reducing crystallinity increases degradation rate in other polymers [31]. It could therefore be expected that PCL network degrades faster than linear PCL, as is indeed the case. However, the difference in the degree of crystallinity does not appear to be enough to explain such a big difference in degradation rate. In this case it seems that hydrophilicity plays a more important role.

3.3 Scanning electron microscopy (SEM)

The SEM microphotographs shown in Fig. 4 suggest differences between the degradation mechanisms of both sample types. Rounded holes, cracks and surface irregularities appeared in PCL network. As degradation proceeded, erosion was more marked in certain areas of the sample while others remained unaltered. In linear PCL the degradation was more uniform and affected the whole surface but not the interior.

These differences indicate that both kinds of samples could follow different degradation mechanisms. It is widely accepted that hydrolytic degradation of poly(α -hydroxy

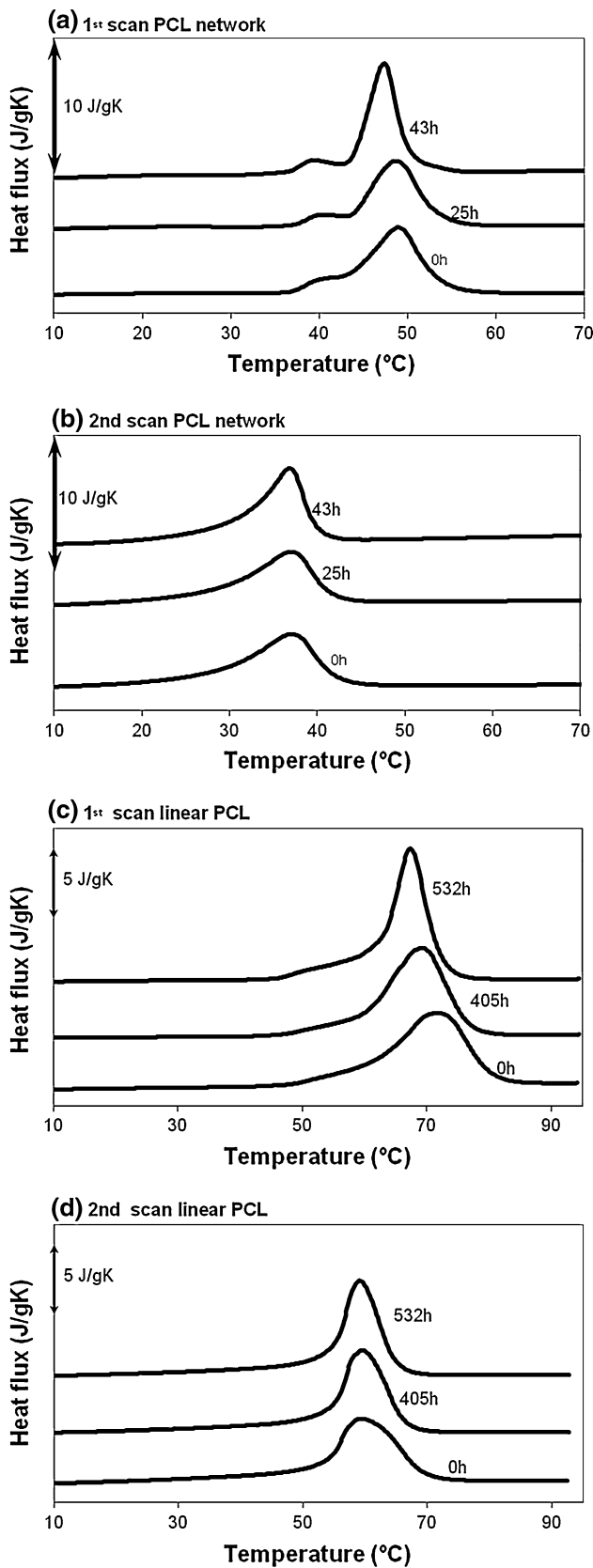


Fig. 3 Heat flux from the first (a) and second (b) heating scans, corresponding to alkaline degradation of PCL network. Heat flux from the first (c) and second (d) heating scans, corresponding to alkaline degradation of linear PCL. Curves are labeled with the corresponding degradation time. The scans have been shifted for better visualization

Table 1 Melting temperature peak and crystallinity measured in the first (T_{m1} , X_1) and second (T_{m2} , X_2) scans for the PCL network as a function of degradation time

| t (h) | $T_{m1} \pm 1$ (°C) | $X_1 \pm 2$ (%) | $T_{m2} \pm 1$ (°C) | $X_2 \pm 2$ (%) |
|-------|---------------------|-----------------|---------------------|-----------------|
| 0 | 49 | 41 | 38 | 33 |
| 9 | 49 | 40 | 36 | 32 |
| 15 | 49 | 41 | 38 | 33 |
| 25 | 49 | 39 | 37 | 31 |
| 28 | 48 | 41 | 37 | 34 |
| 43 | 47 | 43 | 37 | 33 |

Table 2 Melting temperature peak and crystallinity measured in the first (T_{m1} , X_1) and second (T_{m2} , X_2) scans for the linear PCL as a function of degradation time

| t (h) | $T_{m1} \pm 1$ (°C) | $X_1 \pm 2$ (%) | $T_{m2} \pm 1$ (°C) | $X_2 \pm 2$ (%) |
|-------|---------------------|-----------------|---------------------|-----------------|
| 0 | 72 | 56 | 60 | 51 |
| 70 | 70 | 55 | 62 | 49 |
| 188 | 69 | 57 | 60 | 50 |
| 405 | 69 | 57 | 60 | 51 |
| 532 | 68 | 58 | 59 | 50 |

esters) can proceed via surface or bulk-degradation pathways [10]. What determines the means by which degradation takes place is the diffusion–reaction phenomena; when the penetration of water into the material is faster than the hydrolysis rate of ester bonds, degradation is a bulk erosion process. Linear PCL is a hydrophobic polymer and its degradation proceeds via the surface-erosion mechanism, as has been shown previously [2, 3, 20]. On the other hand, the higher hydrophilicity together with lower crystallinity of PCL networks have a considerable effect on degradation rate and bulk degradation is observed.

3.4 Mechanical properties

To evaluate the mechanical properties, stress–strain tests were conducted. For each degradation time, three different samples were measured with three consecutive compression scans. All the measurements show a similar behavior; after a “toe” region, the stress–strain curve shows a linear region, until the maximum stress is reached. When the

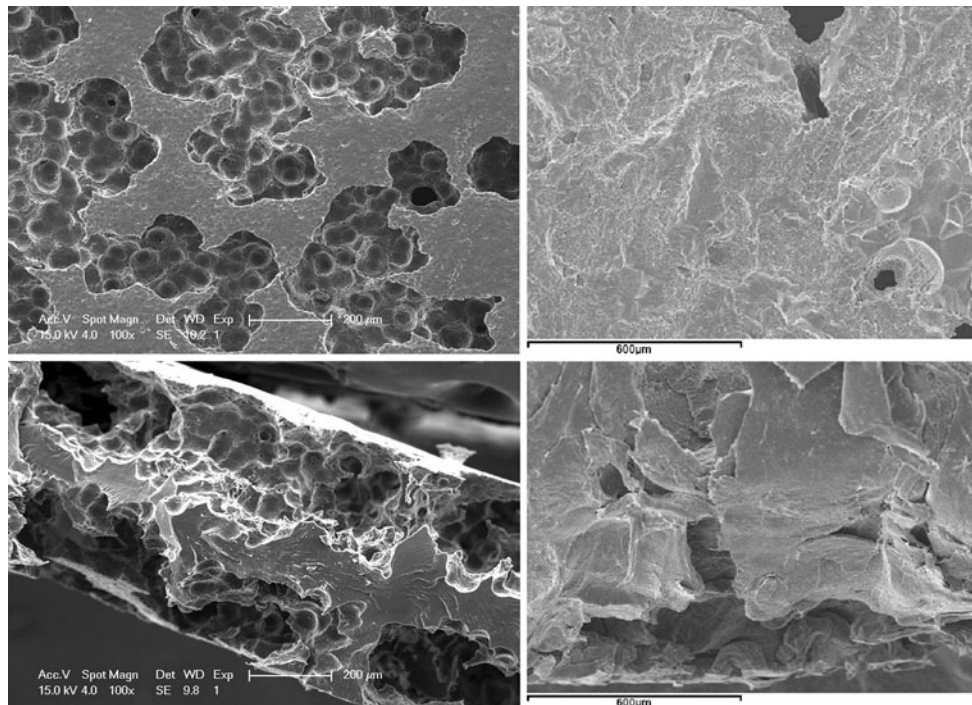


Fig. 4 SEM microphotographs after alkaline degradation. *Left* PCL network after 78.8 h (81% weight loss); *Bar* 200 µm. *Right* linear PCL after 816.8 h (75% weight loss); *Bar* 600 µm. *Top* surface and *bottom* fracture

sample is unloaded, a plastic deformation appears that increases with degradation time. This plastic deformation remains unaltered at the beginning of the third scan. The curves corresponding to the second and third scans are very similar. As an example, the three 22-h compression scans of the degraded PCL network sample are shown on Fig. 5.

To evaluate Young's modulus, the slope of the stress-strain curves in the 4–5 MPa range were chosen. Mean values and standard deviation were calculated for the three samples. Young's modulus values corresponding to first and third compression scans are reported in Tables 3 and 4 for PCL network and linear PCL respectively. Comparison of results before degradation indicates that PCL network

presents lower Young's modulus and higher plastic deformation than linear PCL. This can be explained by the lower crystallinity and glass transition temperature of the

Table 3 PCL network: Young's modulus and plastic deformation for different degradation times

| Degradation time (h) | E_1 (MPa) | Plastic deformation (µm) | E_3 (MPa) |
|----------------------|-------------|--------------------------|-------------|
| 0 | 83 ± 9 | 25 ± 2 | 98 ± 11 |
| 22 | 64 ± 3 | 37 ± 2 | 86 ± 4 |
| 33 | 21 ± 5 | 156 ± 9 | 52 ± 11 |
| 45 | 19 ± 2 | 138 ± 36 | 44 ± 5 |
| 70 | 27 ± 7 | 255 ± 29 | 56 ± 12 |

E_1 corresponds to the Young's modulus calculated in the first scan while E_3 corresponds to the third one

Table 4 Linear PCL: Young's modulus and plastic deformation for different degradation times

| Degradation time (h) | E_1 (MPa) | Plastic deformation (µm) | E_3 (MPa) |
|----------------------|--------------|--------------------------|--------------|
| 0 | 170 ± 30 | $0,8 \pm 2$ | 184 ± 30 |
| 144 | 116 ± 6 | 8 ± 4 | 133 ± 1 |
| 365 | 108 ± 3 | 10 ± 3 | 135 ± 2 |
| 532 | 105 ± 9 | 18 ± 9 | 170 ± 7 |
| 744 | 54 ± 12 | 61 ± 21 | 86 ± 3 |

E_1 corresponds to the Young's modulus calculated in the first scan while E_3 corresponds to the third one

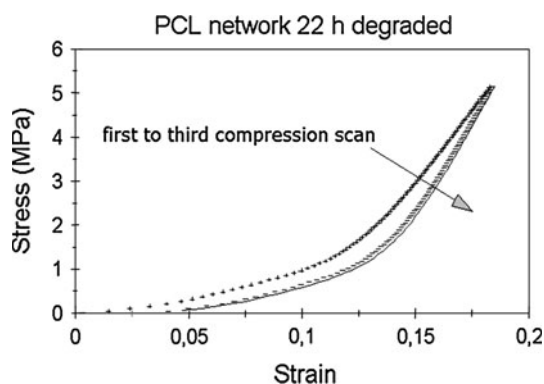


Fig. 5 Stress-strain curves for the PCL network sample 22 h degraded

PCL network samples [28]. As degradation proceeds, the porosity of the samples increases and the elastic modulus decreases, as one would expect [32]. Young's modulus decreases from 83 to 21 MPa after 33 h of degradation for PCL network samples and from 170 to 54 after 744 h of degradation for linear PCL samples. If we compare the mechanical properties as a function of degradation time for both kinds of samples, we find that when PCL network loses 50% of its mass (degradation time equal to 33 h) Young's modulus changes from 83 to 21 MPa (74% of relative variation). The corresponding values for linear PCL (which loses 50% of its mass after 532 h) are 170 and 105 MPa (40% relative variation). The difference can be related to the different degradation mechanisms as previously explained: bulk degradation for the PCL network and surface-erosion mechanism for linear PCL. This produces differences in morphology and porosity and thus in mechanical properties.

The Young's modulus of PCL network samples does not change significantly after 33 h of degradation, indicating that the main part of the degradation process happens during this time interval, with only small changes afterwards. These results are presented not only in the first scan, but also in the third scan and also in the plastic deformation. The values of the Young's modulus measured in the third scan are higher than that in the first, due to the densification effect related to plastic deformation. Therefore, the porosity of the compressed samples is lower and the Young's modulus higher.

4 Conclusions

This paper describes the degradation in NaOH, at 37°C, of poly(ϵ -caprolactone) networks prepared for a new PCL macromer by UV polymerization.

The degradation of PCL network was markedly accelerated, as measured by swelling and weight loss. The weight loss observed in the first 60 h was around 70%, while linear PCL weight loss did not reach 5% in the same period of time. As expected, the higher hydrophilicity of the PCL network as compared with linear PCL causes a higher diffusion of the NaOH in the sample and so a higher degradation rate. The different crystallinity might also have some influence.

Crystallinity in the first heating scan of the non-degraded PCL network is 40%, much lower than that corresponding to linear PCL, which is around 55%. The difference is due to the hampering of crystallization introduced by crosslinking, which restricts chain mobility and thus the polymer's ability to crystallize. There were no appreciable changes in crystallinity throughout degradation either in PCL network or linear PCL. This indicates that

degradation takes place both in the amorphous and crystalline phases simultaneously. In both types of sample the melting peak is observed to shift towards lower temperatures accompanied by a reduction in peak width. This suggests that the degradation process reduces both crystal size and size distribution.

The observed decrease in mechanical properties (Young's modulus and plastic deformation) is due to changes in sample porosity as a consequence of the degradation process. The lower crystallinity of the PCL network samples in comparison with linear PCL could explain the lower values of Young's modulus and higher plastic deformation in these samples.

Accelerated degradation studies were performed primarily to ensure that the PCL network's hydrolytically labile bonds are accessible. From the results it was concluded that the higher hydrophilicity together with lower crystallinity of PCL networks had a considerable effect on degradation rate and bulk degradation was observed. To match the in vivo environment more closely, hydrolytic degradation in phosphate buffer solution and simulated body fluids are now in progress.

Acknowledgments The authors would like to acknowledge the support of the Spanish Ministry of Science and Education through the MEC DPI2007-65601-C03-03 Project. The authors also would like to acknowledge the support of the CIBER-BBN, an initiative funded by the VI National R&D&i Plan 2008–2011, *Iniciativa Ingenio 2010*, *Consolider Program*, *CIBER Actions* and financed by the Instituto de Salud Carlos III with assistance from the *European Regional Development Fund* and the funding by the Centro de Investigación Principe Felipe in the field of regenerative medicine through the collaboration agreement from the Conselleria de Sanidad (Generalitat Valenciana). The translation of this paper was funded by the Universidad Politécnica de Valencia, Spain.

References

1. Hench LL, Polar JM. Third-generation biomedical materials. *Science*. 2002;295:1014–7.
2. Tsuji H, Ishizaka T. Porous biodegradable polyesters. II. Physical properties, morphology, and enzymatic and alkaline hydrolysis of porous poly(ϵ -caprolactone) films. *J Appl Polym Sci*. 2001;80: 2281–91.
3. Ang KC, Leong KF, Chua CK, Chandrasekaran M. Compressive properties and degradability of poly(ϵ -caprolactone)/hydroxyapatite composites under accelerated hydrolytic degradation. *J Biomed Mater Res*. 2007;80A:655–60.
4. Song Y, Liu L, Weng X, Zhuo R. Acid-initiated polymerization of ϵ -caprolactone under microwave irradiation and its application in the preparation of drug controlled release system. *J Biomater Sci Polym Ed*. 2003;14:241–53.
5. Kim HW, Knowles JC, Kim HE. Hydroxyapatite porous scaffold engineered with biological polymer hybrid coating for antibiotic Vancomycin release. *J Mater Sci: Mater Med*. 2005;16: 189–95.
6. Arote R, Kim TH, Kim YK, Hwang SK, Jiang HL, Song HH, Nah JW, Cho MH, Cho CS. A biodegradable poly(ester amine) based

- on polycaprolactone and polyethylenimine as a gene carrier. *Biomaterials*. 2007;28:735–44.
7. Zhong ZK, Sun XZ. Properties of soy protein isolate/polycaprolactone blends compatibilized by methylene diphenyl diisocyanate. *Polymer*. 2001;42:6961–9.
 8. Kweon HY, Yoo MK, Park IK, Kim TH, Lee HC, Lee HS, Oh JS, Akaike T, Cho CS. A novel degradable polycaprolactone networks for tissue engineering. *Biomaterials*. 2003;24:801–8.
 9. Ishaug-Riley SL, Okun LE, Prado G, Applegate MA, Ratcliffe A. Human articular chondrocyte adhesion and proliferation on synthetic biodegradable polymer films. *Biomaterials*. 1999;20:2245–56.
 10. Göpferich A. Mechanisms of polymer degradation and erosion. *Biomaterials*. 1996;17:103–14.
 11. Más Estelles J, Vidaurre A, Meseguer Dueñas JM, Castilla Cortazar MI. Physical characterization of polycaprolactone scaffolds. *J Mater Sci-Mater Med*. 2008;19:189–95.
 12. Albertsson AC, Varma IK. Recent developments in ring opening polymerization of lactones for biomedical applications. *Biomacromolecules*. 2003;4:1466–86.
 13. Vert M. Aliphatic polyesters: Great degradable polymers that cannot do everything. *Biomacromolecules*. 2005;6:538–46.
 14. Chawla JS, Amiji MM. Biodegradable poly(ϵ -caprolactone) nanoparticles for tumor-targeted delivery of tamoxifen. *Int J Pharm*. 2002;249:127–38.
 15. Hayashi T, Nakayama K, Mochizuki M, Masuda T. Studies on biodegradable poly(hexano-6-lactone) fibers. Part 3. Enzymatic degradation in vitro (IUPAC Technical Report). *Pure Appl Chem*. 2002;74:869–80.
 16. Tisuji H, Mizuno A, Ikada Y. Blends of aliphatic polyesters. III. Biodegradation of solution-cast blends from poly(L-lactide) and poly(ϵ -caprolactone). *J Appl Polym Sci*. 1998;70:2259–68.
 17. Albuerne J, Marquez L, Müller AJ, Raquez JM, Degée P, Dubois P. Hydrolytic degradation of double crystalline PPDx-b-PCL diblock copolymers. *Macromol Chem Phys*. 2005;206:903–14.
 18. Kulkarni A, Reiche J, Hartmann J, Kratz K, Lendlein A. Selective enzymatic degradation of poly(ϵ -caprolactone) containing multi-block copolymers. *Eur J Pharm Biopharm*. 2008;68:46–56.
 19. Pitt CG, Gratzl NM, Kimmel GL, Surles J, Schindler A. Aliphatic polyesters. 2. The degradation of poly(DL-Lactide), poly(epsilon-caprolactone) and their copolymers in vivo. *Biomaterials*. 1981;2:215–20.
 20. Vidaurre A, Meseguer Dueñas JM, Más Estellés J, Castilla Cortázar MI. Influence of enzymatic degradation on physical properties of poly(ϵ -caprolactone) films and sponges. *Macromol Symp*. 2008;269:38–46.
 21. Marten E, Müller R-J, Deckwer W-D. Studies on the enzymatic hydrolysis of polyesters I. Low molecular mass model esters and aliphatic polyesters. *Polym Degrad Stab*. 2003;80:485–501.
 22. Mochizuki M, Hiram M. Structural effects on the biodegradation of aliphatic polyesters. *Polym Adv Technol*. 1997;8:203–9.
 23. Li S, Liu L, Garreau H, Vert M. Lipase-catalyzed biodegradation of poly(ϵ -caprolactone) blended with various polylactide-based polymers. *Biomacromolecules*. 2003;4:372–7.
 24. Liu L, Li S, Garreau H, Vert M. Selective enzymatic degradations of poly(L-lactide) and poly(ϵ -caprolactone) blend films. *Biomacromolecules*. 2000;1:350–9.
 25. Pitt CG, Chasalow FI, Hibionada YM, Klimas DM, Schindler A. Aliphatic polyesters. I. The degradation of poly(epsilon-caprolactone) in vivo. *J Appl Polym Sci*. 1981;26:3779–87.
 26. Sun H, Mei L, Song C, Cui X, Wang P. The in vivo degradation, absorption and excretion of PCL-based implant. *Biomaterials*. 2006;27:1735–40.
 27. Bat E, Plantinga JA, Harmsen MC, van Luyn MJA, Zhang Z, Grijpma DW, Feijen J. Trimethylene carbonate an (ϵ -caprolactone) based (co)polymer networks: mechanical properties and enzymatic degradation. *Biomacromolecules*. 2008;9:3208–15.
 28. Escobar Ivirico JL, Salmeron Sanchez M, Sabater i Serra R, Meseguer Dueñas JM, Gomez Ribelles JL, Monleón Pradas M. Structure and properties of poly(ϵ -caprolactone) networks with modulated water uptake. *Macromol Chem Phys*. 2006;207:2195–205.
 29. Sabater i Serra R, Escobar Ivirico JL, Meseguer Dueñas JM, Andrio Balado A, Gomez Ribelles JL, Salmeron Sanchez M. Dielectric relaxation spectrum of poly(ϵ -caprolactone) networks hydrophilized by copolymerization with 2-hydroxyethyl acrylate. *Eur Phys J E*. 2007;22:293–302.
 30. Strobel G. The physics of polymers. Berlin: Springer; 1997. p. 160–90.
 31. Boxberg Y, Schnabelrauch M, Vogt S, Salmerón Sánchez M, Gallego Ferrer G, Monleón Pradas M, Suay Antón JJ. Effect of hydrophilicity on the properties of a degradable polylactide. *J Polym Sci B: Polym Phys*. 2006;44:656–64.
 32. Gibson LJ, Ashby MF. Cellular solids: structure and properties. 2nd ed. Cambridge: Cambridge University Press; 1997.